Spectrochimica Acta Part A: Molecular and Biomolecular Spectroscopy 137 (2015) 70–74

Contents lists available at ScienceDirect

Spectrochimica Acta Part A: Molecular and Biomolecular Spectroscopy

journal homepage: www.elsevier.com/locate/saa

# A vibrational spectroscopic study of the silicate mineral harmotome – $(Ba,Na,K)_{1-2}(Si,Al)_8O_{16}\cdot 6H_2O$ – A natural zeolite

Ray L. Frost [a,*], Andrés López [a], Lina Wang [a,b], Antônio Wilson Romano [c], Ricardo Scholz [d]

[a] School of Chemistry, Physics and Mechanical Engineering, Science and Engineering Faculty, Queensland University of Technology, GPO Box 2434, Brisbane, Queensland 4001, Australia
[b] School of Chemistry and Chemical Engineering, Tianjin University of Technology, No. 391, Bin Shui West Road, Xi Qing District, Tianjin, PR China
[c] Geology Department, Federal University of Minas Gerais, Belo Horizonte, MG 31270-901, Brazil
[d] Geology Department, School of Mines, Federal University of Ouro Preto, Campus Morro do Cruzeiro, Ouro Preto, MG 35400-00, Brazil

## HIGHLIGHTS

- We have studied the mineral harmotome $(Ba,Na,K)_{1-2}(Si,Al)_8O_{16}\cdot 6H_2O$.
- It is a natural zeolite.
- Raman and infrared bands are attributed to siloxane stretching and bending vibrations.
- A sharp infrared band at 3731 $cm^{-1}$ is assigned to the OH stretching vibration of SiOH units.

## GRAPHICAL ABSTRACT

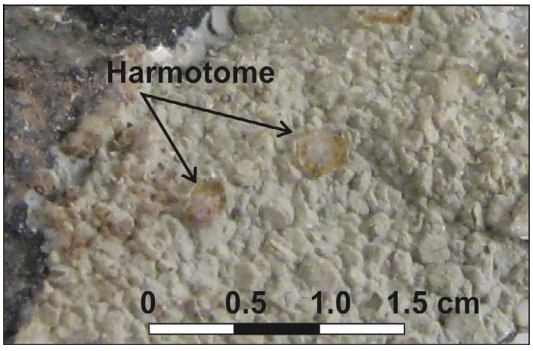


## ARTICLE INFO

*Article history:*
Received 31 March 2014
Received in revised form 7 July 2014
Accepted 28 July 2014
Available online 10 August 2014

*Keywords:*
Harmotome
Zeolite
Barium
Silicate
Raman spectroscopy
Infrared spectroscopy

## ABSTRACT

The mineral harmotome $(Ba,Na,K)_{1-2}(Si,Al)_8O_{16}\cdot 6H_2O$ is a crystalline sodium calcium silicate which has the potential to be used in plaster boards and other industrial applications. It is a natural zeolite with catalytic potential. Raman bands at 1020 and 1102 $cm^{-1}$ are assigned to the SiO stretching vibrations of three dimensional siloxane units. Raman bands at 428, 470 and 491 $cm^{-1}$ are assigned to OSiO bending modes. The broad Raman bands at around 699, 728, 768 $cm^{-1}$ are attributed to water librational modes. Intense Raman bands in the 3100 to 3800 $cm^{-1}$ spectral range are assigned to OH stretching vibrations of water in harmotome. Infrared spectra are in harmony with the Raman spectra. A sharp infrared band at 3731 $cm^{-1}$ is assigned to the OH stretching vibration of SiOH units. Raman spectroscopy with complimentary infrared spectroscopy enables the characterization of the silicate mineral harmotome.



## Introduction

Harmotome is a white mineral, of formula $(Ba,Na,K)_{1-2}(Si,Al)_8O_{16}\cdot 6H_2O$ and may be described as an hydrated barium sodium alumino-silicate [1–3]. It is a naturally occurring zeolite and is often associated with other zeolites. Harmotome is one of the rarer zeolites and is popular among mineral collectors. If perfectly formed, a twinned crystal of harmotome can appear to be composed of three prismatic crystals grown through the each others' center at nearly 90° angles. Please see the image given in Fig. 1.

Harmotome is monoclinic, space group P1 with unit cell of symmetry P21 with a 9.87, b 14.14, c 8.72 A.; β 124°50′ [3]. Harmotome is isostructural with phillipsite [2] [4]. A review of the structure of harmotome and related minerals has been published [5]. The crystal structure was determined at different temperatures by X-ray

* Corresponding author. Tel.: +61 7 3138 2407; fax: +61 7 3138 1804.
*E-mail address:* r.frost@qut.edu.au (R.L. Frost).

http://dx.doi.org/10.1016/j.saa.2014.07.072
1386-1425/

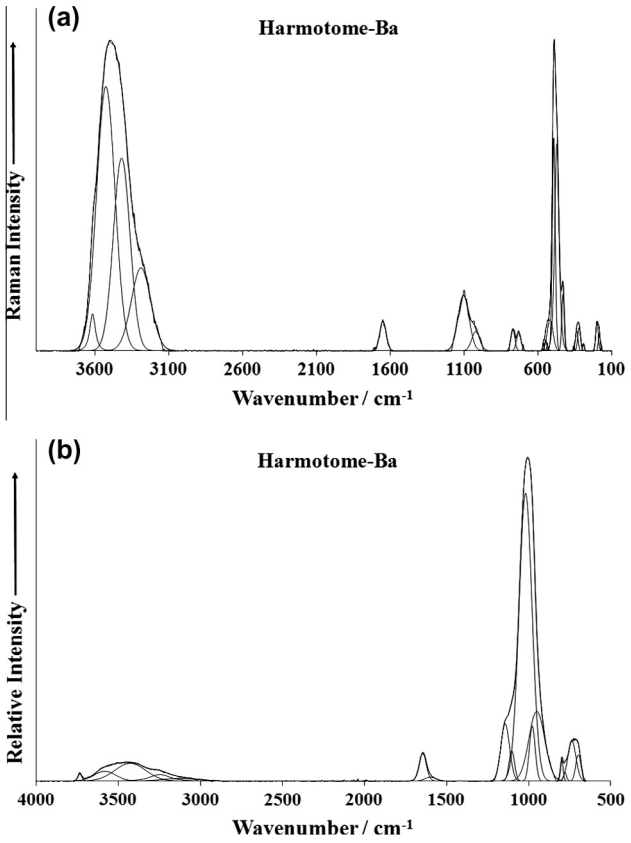


**Fig. 1.** (a) Raman spectrum of harmotome (upper spectrum) over the 100–4000 $cm^{-1}$ spectral range and (b) infrared spectrum of harmotome (lower spectrum) over the 500–4000 $cm^{-1}$ spectral range.

diffraction and neutron diffraction. In the structure of harmotome each barium cation is coordinated by four water molecules (O10, O20, O30).

No Raman spectroscopic studied of harmotome and related minerals have been forthcoming [6]. Some infrared studies have been undertaken [7,8]. Studies of hydrogen bonding in silicates relates the position of the hydroxyl stretching vibration to the hydrogen bond distances [9]. Raman studies of cement phases have been forthcoming [10–13]. Some infrared studies of calcium silicates have been undertaken [14–16]. Some Raman spectra of calcium silicates have been collected and a number of the spectra were shown to be dependent upon the number of condensed silica tetrahedra [12]. Such detailed assignment of infrared and Raman bands for a wide range of silicate structures was made by Dowty [17–20]. The thermal decomposition of calcium silicates has also been measured [21–23]. Harmotome is readily synthesised and is often found as components in cements [24,25]. Harmotome may be used to make reinforced organic polymers. It can be used for the removal of organic polyelectrolytes and their metal complexes by adsorption onto harmotome. Harmotome and related minerals can be used for heavy metal uptake for example Nd(II) [24].

There is an apparent lack of information on the vibrational spectra of harmotome. The reason for such a lack of information is not known; yet the mineral contains water and siloxane units. Such units lend themselves to vibrational spectroscopy. Raman spectroscopy has proven most useful for the study of mineral structure. The objective of this research is to report the Raman and infrared spectra of harmotome and to relate the spectra to the mineral structure.

Harmotome as a building material may have many and varied applications which are based upon the inherent properties of harmotome including porosity, thermal insulation and thermal decomposition temperature. In order to raise the on-set combustion temperature of plaster boards, new types of plaster boards are made by combining gypsum with harmotome. As part of this research, we have undertaken a vibrational spectroscopic study of harmotome to determine the characteristic bands of this mineral.

## Experimental

### *Samples description and preparation*

The harmotome sample studied in this work occurs as single crystals with tabular habitus up to 5 cm. The sample is part of the collection of the Geology Department of the Federal University of Ouro Preto, Minas Gerais, Brazil, with sample code SAD-012. The mineral sample originated from Mannbühl Quarry (Giro Quarry), Dannenfels, Kirchheimbolanden, Rhineland-Palatinate, Germany [26,27]. Harmotome occurs in centimetric distension cavities in a mineralized fault in dacite, in association with calcite. The sample was gently crushed and the associated minerals were removed under a stereomicroscope Leica MZ4. The harmotome sample studied in this work was analyzed by scanning electron microscopy (SEM) in the EDS mode to support the mineral characterization.

### *Scanning electron microscopy (SEM)*

Experiments and analyses involving electron microscopy were performed in the Center of Microscopy of the Universidade Federal de Minas Gerais, Belo Horizonte, Minas Gerais, Brazil (http://www.microscopia.ufmg.br). Harmotome crystals were coated with a 5 nm layer of evaporated carbon. Secondary Electron and Backscattering Electron images were obtained using a JEOL JSM-6360LV equipment. Qualitative and semi-quantitative chemical analyses in the EDS mode were performed with a ThermoNORAN spectrometer model Quest and were applied to support the mineral characterization.

### *Raman microprobe spectroscopy*

Crystals of harmotome were placed on a polished metal surface on the stage of an Olympus BHSM microscope, which is equipped with 10×, 20×, and 50× objectives. The microscope is part of a Renishaw 1000 Raman microscope system, which also includes a monochromator, a filter system and a CCD detector (1024 pixels). The Raman spectra were excited by a Spectra-Physics model 127 He–Ne laser producing highly polarized light at 633 nm and collected at a nominal resolution of 2 $cm^{-1}$ and a precision of ±1 $cm^{-1}$ in the range between 200 and 4000 $cm^{-1}$. Repeated acquisitions on the crystals using the highest magnification (50×) were accumulated to improve the signal to noise ratio of the spectra. Raman Spectra were calibrated using the 520.5 $cm^{-1}$ line of a silicon wafer.

### *Infrared spectroscopy*

Infrared spectra of harmotome were obtained using a Nicolet Nexus 870 FTIR spectrometer with a smart endurance single bounce diamond ATR cell. Spectra over the 4000–525 $cm^{-1}$ range were obtained by the co-addition of 128 scans with a resolution of 4 $cm^{-1}$ and a mirror velocity of 0.6329 cm/s. Spectra were co-added to improve the signal to noise ratio. The infrared spectra are given in the Supplementary information.

Spectral manipulation such as baseline correction/adjustment and smoothing were performed using the Spectracalc software package GRAMS (Galactic Industries Corporation, NH, USA). Band component analysis was undertaken using the Jandel 'Peakfit' software package that enabled the type of fitting function to be selected and allows specific parameters to be fixed or varied

accordingly. Band fitting was done using a Lorentzian–Gaussian cross-product function with the minimum number of component bands used for the fitting process. The Gaussian–Lorentzian ratio was maintained at values greater than 0.7 and fitting was undertaken until reproducible results were obtained with squared correlations of $r^2$ greater than 0.995.

## Results and discussion

### *Mineral characterization*

The SEM image of harmotome sample studied in this work is provided as Supplementary information in Fig. S1. The image shows a cleavage fragment up to 2 mm. Qualitative chemical analysis shows a homogeneous phase, composed by Ba, Al, Na, K and Si. No other contaminant elements were observed and the sample can be considered as a pure single phase (Supplementary information Fig. S2).

### *Vibrational spectroscopy*

The Raman spectrum of harmotome over the 100–4000 $cm^{-1}$ spectral range is shown in Fig. 1a. This figure shows the position and relative intensity of the Raman bands. It is noted there are large parts of the spectrum where little or no intensity is observed. The Raman spectrum is therefore subdivided into sections based upon the types of vibration being studied. The infrared spectrum of harmotome over the 500–4000 $cm^{-1}$ spectral range is displayed in Fig. 1b. This figure shows the position and relative intensities of the infrared bands. The infrared spectrum is subdivided into sections based upon the type of vibration being analyzed.

The Raman spectrum of harmotome over the 950–1750 $cm^{-1}$ spectral range is reported in Fig. 2a. The structure of harmotome consists of three dimensional silicates with multiple linked silica tetrahedra [28]. Two Raman bands are observed at 1020 and 1102 $cm^{-1}$ and are assigned to the SiO stretching vibrations. The Raman band at 1648 $cm^{-1}$ with a shoulder at 1707 $cm^{-1}$ is assigned to water bending vibrational mode. Dowty calculated the band positions for the different ideal silicate units. Dowty showed that the -$SiO_3$ units had a unique band position of 1025 $cm^{-1}$ [20] (see Figs. 2 and 4 of this reference). Dowty calculated the Raman spectrum for these type of silicate networks and predicted two bands at around 1040 and 1070 $cm^{-1}$ with an additional band at around 600 $cm^{-1}$. The Raman spectrum of harmotome is given in the RRUFF data base. The spectrum is provided in the Supplementary information (Fig. S3). This RRUFF spectrum shows a very broad band at 1107 $cm^{-1}$. There is also a very low intensity band at around 1000 $cm^{-1}$. These bands are in harmony with the Raman bands of harmotome reported in this work.

The infrared spectrum over the 650–1250 $cm^{-1}$ spectral range is reported in Fig. 2b. The infrared spectrum is quite broad and may be resolved into component bands at 947, 976, 1016, 1100 and 1140 $cm^{-1}$. These bands are assigned to SiO stretching vibrations. The infrared band at 1016 $cm^{-1}$ is the equivalent of the Raman band at 1020 $cm^{-1}$ and the infrared band at 1100 $cm^{-1}$ is the infrared equivalent of the Raman band at 1102 $cm^{-1}$. The series of infrared bands at 694, 733, 775 and 795 $cm^{-1}$ are considered to be due to water librational modes.

These bands are observed in the Raman spectrum (Fig. 3a) at 699, 728 and 768 $cm^{-1}$. In the RRUFF Raman spectrum, bands are found at 616, 726 and 770 $cm^{-1}$. Intense Raman bands of harmotome are observed at 470 and 591 $cm^{-1}$ and are assigned to OSiO bending vibrations. Bands of lesser intensity are observed at 428, 534, 546 and 561 $cm^{-1}$. These bands may also be attributed to this vibrational mode. The most intense band in the RRUFF Raman

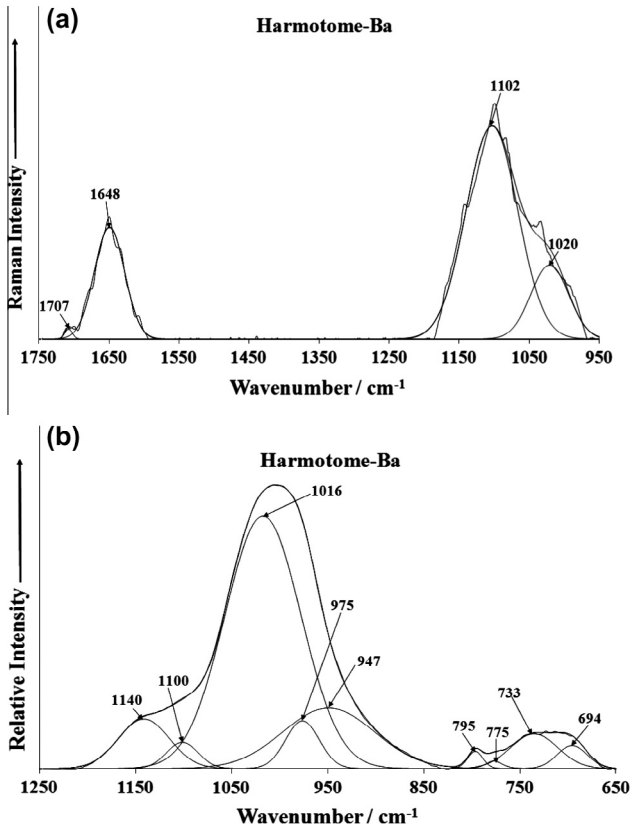


**Fig. 2.** (a) Raman spectrum of harmotome over the 950–1750 $cm^{-1}$ spectral range and (b) infrared spectrum of harmotome over the 650–1250 $cm^{-1}$ spectral range.

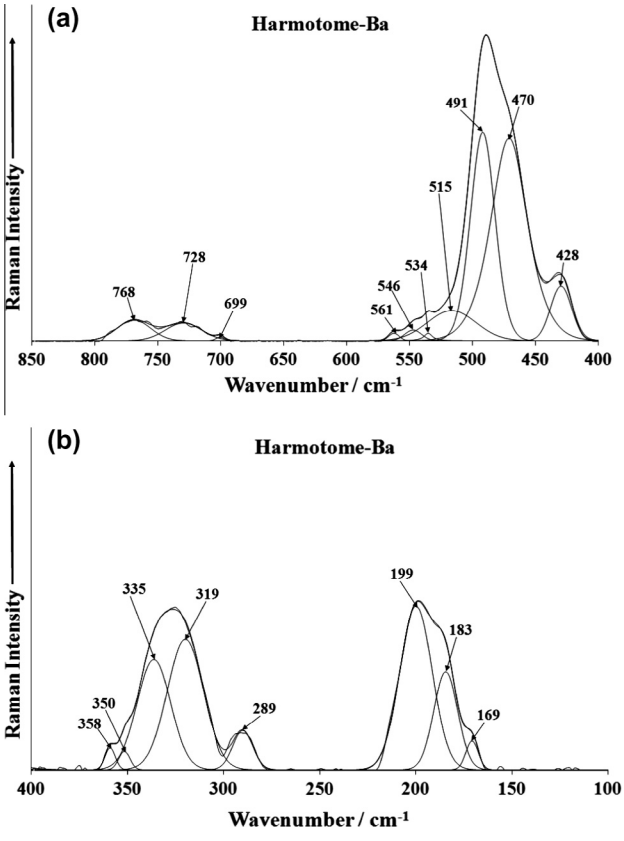


**Fig. 3.** (a) Raman spectrum of harmotome (upper spectrum) in the 400–850 $cm^{-1}$ spectral range and (b) Raman spectrum of harmotome (lower spectrum) in the 100–400 $cm^{-1}$ spectral range.

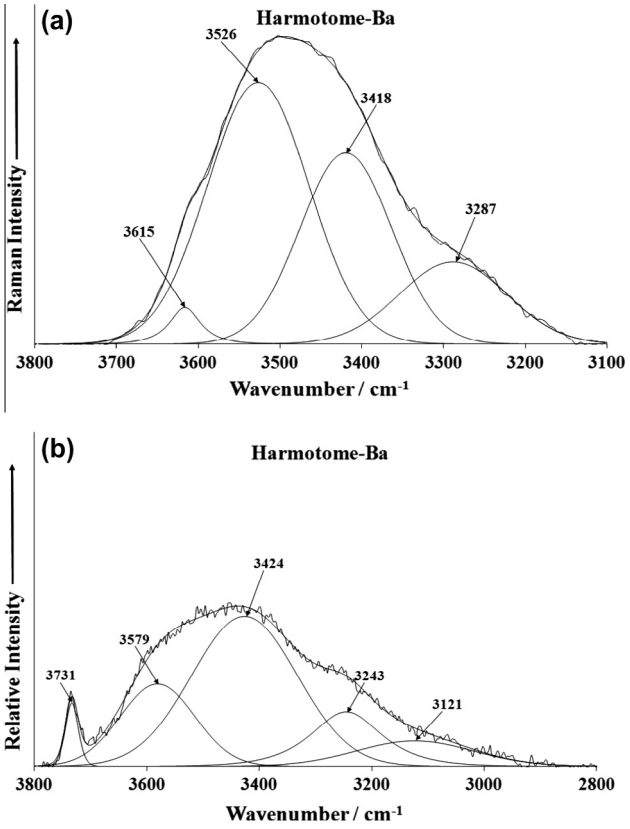


**Fig. 4.** (a) Raman spectrum of harmotome over the 3100–3800 $cm^{-1}$ spectral range and (b) infrared spectrum of harmotome over the 2800–3800 $cm^{-1}$ spectral range.

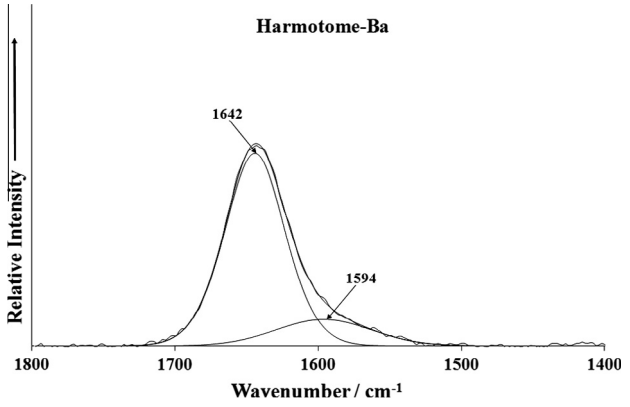


**Fig. 5.** Infrared spectrum of harmotome over the 1400–1800 $cm^{-1}$ spectral range.

spectrum (Fig. S1) is a band at 487 $cm^{-1}$. This observation is in harmony with the bands noted in this work. A series of Raman bands are found at 289, 319, 335 350 and 358 $cm^{-1}$. These bands are attributed to metal oxygen stretching vibrations (BaO) (Fig. 3b). Other Raman bands are observed at 169, 183 and 199 $cm^{-1}$ and are simply described as lattice vibrations.

The Raman spectrum of harmotome in the 3100 and 3800 $cm^{-1}$ is reported in Fig. 4a. Intense bands are observed in the Raman spectrum. The Raman spectrum is very broad; however the spectral profile may be resolved into component bands at 3287, 3418, 3526 and 3615 $cm^{-1}$. These bands are assigned to the water stretching bands of water in harmotome. The range of peak positions provides evidence for a range of hydrogen bond strengths in the structure of harmotome. The infrared spectrum of harmotome over the 2800–3800 $cm^{-1}$ spectral region is shown in Fig. 4b. The infrared spectrum is quite broad. The spectral profile may be resolved into component bands at 3121, 3243, 3424 and 3579 $cm^{-1}$. These bands are assigned to water stretching vibrations. In addition, a sharp infrared band is noted at 3731 $cm^{-1}$. This band is assigned to the OH stretching vibration of SiOH units. Both Raman and infrared bands at around 3400 $cm^{-1}$ are attributed to strong hydrogen bonding. The hydrogen bond distance is short. Such a range of hydrogen bond strengths is also reflected in the water bending modes (Fig. 5) where the band at 1642 $cm^{-1}$ with a broad band at lower wavenumbers at 1594 $cm^{-1}$ is observed. This former band is attributed to the water bending modes of water involved in strong hydrogen bonding.

## Conclusions

The Raman spectrum of harmotome is characterized by intense broad bands at 1020 and 1102 $cm^{-1}$. These bands are assigned to the SiO stretching vibrations of the $(Si,Al)_8O_{16}$ units. Strong infrared bands are found at 1016 and 1140 $cm^{-1}$ and are attributed to SiO stretching vibrations. Intense Raman bands at 428, 470 and 491 $cm^{-1}$ are assigned to OSiO bending vibrations. The intense Raman band profile centered upon ~3500 $cm^{-1}$ is attributed to the OH stretching vibrations of water units in the harmotome structure. The infrared spectrum shows a very broad band centered upon 3424 $cm^{-1}$ with component bands at 3243, 3424, 3579 $cm^{-1}$ attributed to water stretching vibrations. A sharp infrared band at 3731 $cm^{-1}$ is assigned to SiOH stretching vibration. This band is not observed in the Raman spectrum. The mineral harmotome is well and truly characterized by its Raman spectrum. Further, Raman spectroscopy offers a technique for the study of harmotome and its admixtures including gypsum. As part of this research, we have undertaken a vibrational spectroscopic study of harmotome to determine the characteristic bands of this mineral.

## Acknowledgements

The financial and infra-structure support of the Discipline of Nanotechnology and Molecular Science, Science and Engineering Faculty of the Queensland University of Technology, is gratefully acknowledged. The Australian Research Council (ARC) is thanked for funding the instrumentation. The authors would like to acknowledge the Center of Microscopy at the Universidade Federal de Minas Gerais (http://www.microscopia.ufmg.br) for providing the equipment and technical support for experiments involving electron microscopy.

## Appendix A. Supplementary material

Supplementary data associated with this article can be found, in the online version, at http://dx.doi.org/10.1016/j.saa.2014.07.072.

## References

[1] R.M. Barrer, F.W. Bultitude, I.S. Kerr, J. Chem. Soc. (1959) 1521–1528.
[2] H. Hoss, R. Roy, Beitr. Mineral. u. Petrog. 7 (1960) 389–408.
[3] R. Sadanaga, F. Marumo, Y. Takeuchi, Acta Cryst. 14 (1961) 1153–1163.
[4] C.T. Prewitt, M.J. Buerger, Min. Soc. Amer. Special Paper, No. 1, 1963, pp. 293–302.
[5] N.V. Belov, Min. Sbornik (Lvov) (1960) 3–33.
[6] C.L. Knight, M.A. Williamson, R.J. Bodnar, Microbeam Analysis (San Francisco) (1989) 571–573. 24th.
[7] I.A. Belitskii, G.A. Golubova, Mater. Genet. Eksper. Min. 7 (1972) 310–323.
[8] F. Pechar, D. Rykl, Casopis pro Min. Geol. 26 (1981) 143–156.
[9] E. Libowitzky, Monat. fuer Chem. 130 (1999) 1047–1059.
[10] L. Black, Spectrosc. Prop. Inorg. Organomet. Compd. 40 (2009) 72–127.
[11] L. Black, C. Breen, J. Yarwood, J. Phipps, G. Maitland, Adv. App. Cer. 105 (2006) 209–216.
[12] W. Pilz, Acta Phys. Hung. 61 (1987) 27–30.
[13] I.G. Richardson, J. Skibsted, L. Black, R.J. Kirkpatrick, Adv. Cement Res. 22 (2010) 233–248.
[14] O. Henning, B. Gerstner, Wissenschaftliche Zeit. Hoch. 19 (1972) 287–293.

[15] G.M. Krylov, Y.M. Priev, Dok. Akad. Nauk USSR (1959) 25–27.
[16] G.M. Krylov, G.F. Sirotenko, Dok. Akad. Nauk USSR (1961) 41–44.
[17] L. Ancillotti, E.M. Castellucci, M. Becucci, Proc. SPIE-Int. Soc. Opt. Eng. 58 (2005) 182–189.
[18] E. Dowty, Phys. Chem. Min. 14 (1987) 542–552.
[19] E. Dowty, Phys. Chem. Min. 14 (1987) 122–138.
[20] E. Dowty, Phys. Chem. Min. 14 (1987) 80–93.
[21] Y. Okada, H. Shibasaki, T. Masuda, Onoda Kenkyu Hokoku 45 (1994) 126–141.
[22] A. Winkler, W. Wieker, Zeit. Chem. 18 (1978) 375–376.
[23] A.E. Zadov, N.V. Chukanov, N.I. Organova, O.V. Kuz'mina, D.I. Belokovskii, M.A. Litsarev, V.G. Nechai, F.S. Sokolovskii, Zap. Vser. Min. Obsh. 130 (2001) 26–40.
[24] S. Komarneni, D.M. Roy, A. Kumar, Mater. Res. Soc. Symp. Proc. 44 (1985) 927–934.
[25] H. Noma, Y. Adachi, H. Yamada, Y. Matsuda, T. Yokoyama, Inter. Ceramic Mono. 2 (1996) 2450–2458.
[26] K. Kohout, Lapis 33 (2008) 32–35.
[27] R. Bungert, W.G. Frey, P. Hesse, Lapis 33 (2008) 13–19.
[28] E. Thilo, H. Funk, Zeit. Anorgan. Chem. 262 (1950) 185–191.